Adsorption and Self-limiting Mechanisms of Trimethylaluminum and Water on Aluminum Oxide Surface

Masashi OZEKI[1)], Tomohiro HARAGUCHI[2)], Keisuke HIRAKAWA[3)], Kohei UWAI[3)]

ABSTRACT

The adsorption processes of $(CH_3)_3Al$ (TMA) and H_2O on γ-Al_2O_3 have been studied to obtain the basic data on the self-limiting mechanism in the atomic layer epitaxy (ALE). The reactant species, TMA and H_2O, were transported onto heated Al_2O_3 surface with the hydrogen carrier gas. The adsorption rate, as a function of the surface coverage of aluminum or oxygen, was estimated from the reactant exposure-time dependence of the deposition thickness of γ-Al_2O_3. The aluminum and oxygen coverage dependence of the adsorption rate suggested that the TMA and H_2O were adsorbed by a precursor-mediated mechanism. The ALE of γ-Al_2O_3 was investigated on the basis of the adsorption data. The self-limiting mechanism, which automatically stopped the growth at just one monolayer of γ-Al_2O_3 (001), was observed in the TMA and H_2O exposure-duration dependences. A growth model of the γ-Al_2O_3 ALE successfully explained the growth rate.

Keywords:
Atomic-layer-epitaxy; Self-limiting mechanism; γ-Al_2O_3; Adsorption

1. INTRODUCTION

Aluminum oxide (Al_2O_3) is widely used as an insulating material in various electronic devices. Recent nanotechnology needs the atomic-order thin film of Al_2O_3 for metal/insulator/semiconductor (MIS) devices [1-3]. Atomic layer epitaxy (ALE), which grows the film in an atomic-order, is suitable for such a thin film growth [4]. ALE has a unique growth mechanism called a self-limiting mechanism (SLM) in the growth rate. This mechanism enables the film growth to stop automatically at exactly n monolayer (n is usually an integer).

SLM has been realized by the tailor-made control of the chemical reactions between the precursor and the crystal surface. Let's consider the following simple ALE of the crystal AB (A: cation and B: anion). (1) The cation source AX (X: CH_3, Cl, etc.) is first absorbed into a mobile, weakly bound precursor state. (2) The dissociation of AX occurs as it encounters the reaction site such as the surface step. The surface is terminated with the cations (Fig. 1(a)). (3) Once the surface is completely covered with cations, the further reaction between the AX and the surface is limited by SLM and therefore the growth stops in this step (Fig. 1(b)). (4) Next, the anion source BY (Y: CH_3, Cl, etc.) is supplied on the cation-terminated surface and is adsorbed on the surface. (5) The surface again changes by the reaction with the BY (Fig. 1(c)). (6) The further reaction between the surface and the BY is again limited on the anion-terminated surface (Fig. 1(d)). In the reaction sequence from step (1) to step (6), which is called "1 cycle", the one monolayer of the compound AB is grown.

The ALE has been reported for the growths of various semiconductor crystals [5-9]. In many semiconductor crystals, the bonds are covalent and their crystal structures are relatively simple. Fig. 2(a) shows the schematic representation of the unit cell of GaAs which is a typical semiconductor and has a zinc blend structure. In the figure, the arsenic atoms occupy the vertices of the tetrahedron and the gallium atoms the center of the tetrahedron. In the ALE of GaAs, the SLM was observed just at one monolayer (the thickness. 0.28 nm equals to the half of the

1) Prof., Electrical and Electronic Engineering
2) Technical Staff, Technical Center, Faculty of Engineering
3) Student, Electrical and Electronic Engineering

lattice constant, 0.56 nm) for the 1 cycle of source supply. On the other hand, Al_2O_3 has a complex structure as shown in Fig. 2(b) and the bond is ionic rather than covalent. γ-Al_2O_3 has a spinel-like structure with Al cations occupying the Al and Mg sites in magnesium spinel (MgO, Al_2O_3) [10]. In this crystal, the oxygen atoms form a face-centered cubic lattice and occupy the vertices of the tetrahedron and the octahedron in the figure. The aluminum atoms occupy the center of the tetrahedron and the octahedron and some of them are indicated as small circles in the figure. Due to the complex structure, a more sophisticated control would be necessary to realize the SLM of γ-Al_2O_3 than that of GaAs.

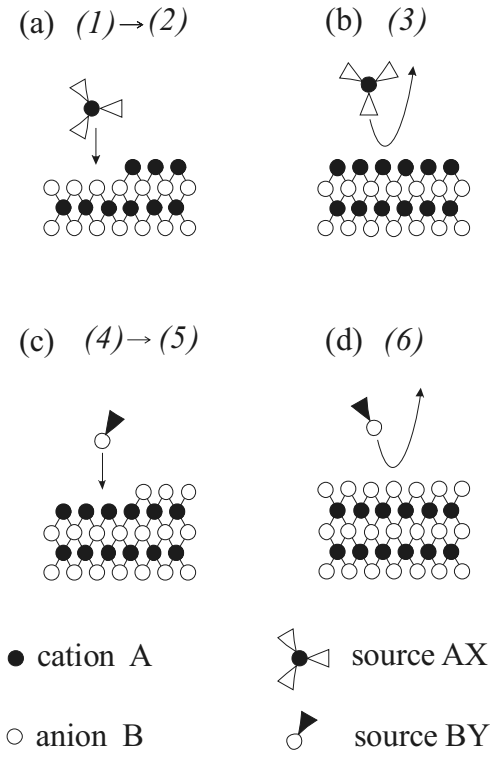

Fig.1 ALE process (a) The AX adsorbs and migrates on the surface to dissociate into A and X. A is incorporated into the surface layer. (b) Once the surface was covered with the A, the additional AX cannot react with the surface. (c) The BY reacts with the surface terminated with A, and B is incorporated into the surface layer. (c) Once the surface was covered with the B, the additional BY cannot react with the surface.

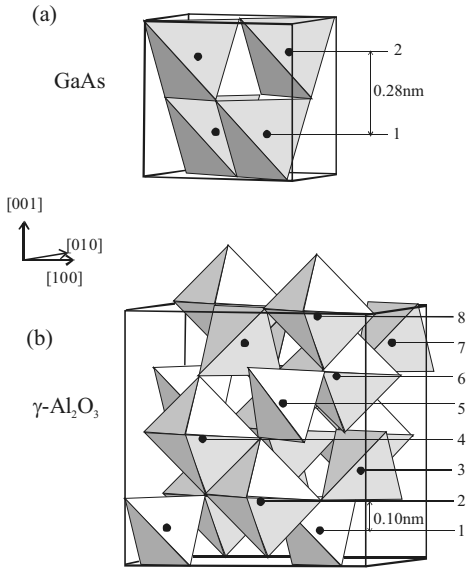

Fig. 2 Schematic representation of the crystal structures of GaAs and γ-Al_2O_3. The anions and cations occupy the vertices and the center of the tetrahedron and the octahedron, respectively. The cubic represents the unit cell but all the atoms are not described.

Some works on the Al_2O_3 growth have been done using the atomic-layer-deposition (ALD) where the deposition was carried out at low temperatures below 500 °C and therefore the deposited Al_2O_3 film was not single crystal but polycrystals [11-14]. The ALD also uses the alternative supply of source molecules as in the ALE but does not involve the SLM in the growth process. The purpose of this study was to get the basic information on the adsorption mechanisms of the TMA and the H_2O on the Al_2O_3 surface in order to develop the ALE technique for single crystal of Al_2O_3 ALE.

2. EXPERIMENTAL

The adsorption mechanisms of $(CH_3)_3Al$ (trimethylaluminum: TMA) and H_2O on the γ-Al_2O_3 surface were investigated in a pulsed-jet type reactor, where the source molecules were introduced from a jet nozzle with the carrier gas hydrogen and injected onto the crystal surface [8]. The pressure of the reactor was 15.0 Torr. The jet flow prevented the thermal decomposition of source molecules in the gas phase and the non-reacted molecules were immediately evacuated from the reactor

with high capacity vacuum pumps. TMA easily decomposes into aluminum and hydrocarbon above 500 °C and has been used as an important source for the deposition of the aluminum-containing film. The behavior of TMA on the oxygen-terminated Al_2O_3 surface is now unknown, but the authors assumed from the analogies of TMA on GaAs surface that it dissociated through a precursor-mediated reaction, where the TMA physisorbed and migrated on the surface and some TMA molecules dissociated on the reaction sites and the other ones desorbed from the surface without any dissociations (Fig. 3).

The adsorption rate of the TMA on the oxygen terminated Al_2O_3 was obtained by the following procedure (Fig. 4). After the Al_2O_3 surface was exposed to H_2O for 10 s in order to terminate the surface with oxygen, the surface was exposed to TMA for the duration t_{TMA} [s]. In this process (one cycle), the aluminum and oxygen were deposited and the new surface layer was formed. The deposition thickness d_{depo} [nm] was monitored by the optical ellipsometer and plotted as a function of t_{TMA} as shown in Fig. 4(b). The adsorption rate of TMA, R_{ads}^{TMA} [s^{-1}], was assumed to be proportional to the deposition rate $\Delta d_{depo} / \Delta t_{TMA}$ [nm s^{-1}] which was the gradient of the d_{depo}–t_{TMA} plot in Fig. 4(b), and was defined as

$$R_{ads}^{TMA} = \frac{\Delta d_{depo}}{\Delta t_{TMA}} \times \frac{1}{d_{layer}} \times \frac{N_{Al}}{N_{coll}} \quad , \qquad (1)$$

Here N_{Al} [atom cm^{-2}] was the surface density of aluminum of the γ-Al_2O_3, d_{layer} [nm] the one monolayer thickness, and N_{coll} [molecules cm^{-2} s^{-1}] the number of the reactant colliding the surface. If the gas temperature T (in degrees Kelvin) near the surface is assumed to be equal to the surface one, N_{coll} is given by

$$N_{coll} = 5.8 \times 10^{-2} \, p \frac{N_A}{\sqrt{MT}} \quad , \qquad (2)$$

where p (in Torr) is the partial pressure of the reactant, M the molecular weight, and N_A the Avogadro number. Using the same procedure, the adsorption rate of H_2O, $R_{ads}^{H_2O}$ [s^{-1}], was obtained from the H_2O exposure duration dependence of d_{depo}.

Based on the basic data on the adsorption, the SLM in the Al_2O_3 ALE was studied using TMA and H_2O. GaAs(001) was used for the initial substrate, since the Al_2O_3/GaAs(001) structure was important in the device application. The Al_2O_3 was located on a RF-heated carbon block in the pulsed-jet reactor. The surface structure of the grown film was measured by the reflection-high-energy-electron-diffraction (RHEED) after the growth. The film thickness was obtained by the high-resolution scanning-electron-microscopy (HR-SEM) measurement of the cleaved (110) face. The growth rate of Al_2O_3 was calculated by dividing the film thickness by the number of the gas-cycle.

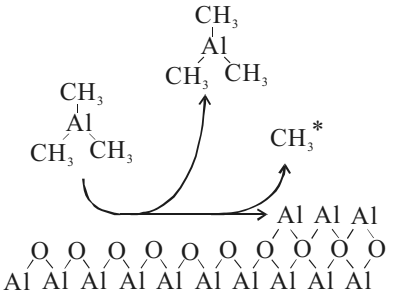

Fig. 3 Simple diagram of the growth of Al_2O_3. TMA is first physisorbed on the oxygen terminated surface and reacts (chemisorbs) on the reaction site. Non-reacted TMA again desorbs from the surface.

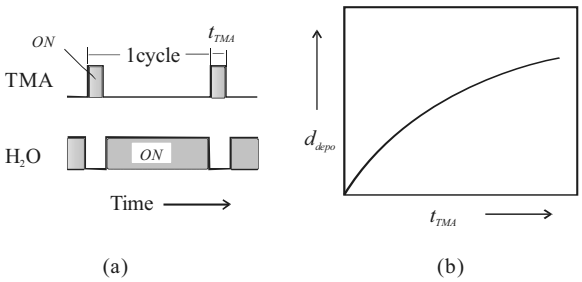

Fig. 4 Schematic diagram of the time sequence of TMA and H_2O exposures (a) and the TMA exposure dependence of the deposition thickness of γ-Al_2O_3 (b).

3. RESUILTS AND DISCUSSIONS

3.1. Adsorption rates of TMA and H_2O

The adsorption of TMA was studied for the (001) face of the single crystalline γ-Al_2O_3. The surface temperature of γ-Al_2O_3 was 1023 K. The mole fraction of TMA was 2.2×10^{-4} (the carrier gas: H_2). If the gas temperature near the surface is assumed to be equal to the surface temperature, the number of the TMA molecules colliding the surface is estimated to be 3.9×10^{17} molecules cm^{-2} s^{-1} from Eq. (2). Before the adsorption process of TMA, Al_2O_3 surface was exposed to the H_2O with the mole fraction of 2.0×10^{-4} and a sufficiently long duration (10 s); this H_2O exposure

corresponded to the surface collision of 7.7×10^{18} molecules cm^{-2}.

Fig. 5 shows the deposition rate as a function of deposition thickness d_{depo}. It should be noted that the Al surface coverage s_{Al} is related to d_{depo} and be expressed in the unit of "monolayer" by

$$s_{Al} = \frac{d_{depo}}{d_{layer}}. \quad (3)$$

The aluminum atoms are distributed to eight layers (four high-density layers and four low-density layers) along <001> direction in the γ-Al_2O_3 unit cell. Therefore, d_{layer} was approximated by (the lattice constant a_0) / 8 = 0.794 / 8 ≅ 0.10 nm on the assumption that the distances between layers were the same d_{layer}.

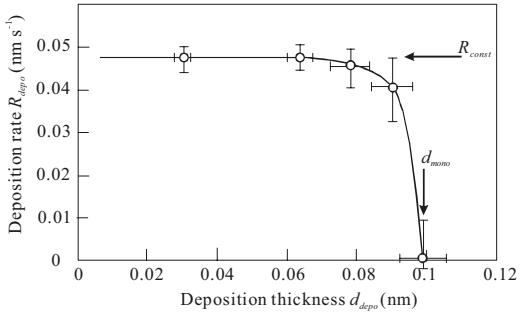

Fig. 5 Deposition thickness dependence of the deposition rate of aluminum. The deposition rate kept constant below the deposition of 0.08 nm but drastically dropped to zero at the thickness of d_{mono}.

The adsorption rate R_{ads} was estimated from the deposition rate R_{depo} as mentioned in the experimental section. The R_{ads} is proportional to the deposition rate R_{depo} from Eq. (1). The deposition rate kept a constant value R_{const} = 0.048 nm s^{-1} up to the deposition thickness of 0.08 nm and then drastically decreased to zero at d_{mono} = 0.10 nm. This variation suggested that the aluminum atoms were incorporated into the surface layer through the precursor-mediated adsorption. In this adsorption mechanism, the precursors of aluminum freely move on the growing surface until they find the vacant adsorption site to react there (chemisorption). The non-reacted TMA molecules desorb from the surface into the gas phase. The drop of R_{depo} to nearly zero at the deposition thickness d_{mono} suggested that the new surface was inactive for TMA at d_{mono} and therefore the ALE with an effective SLM, which stopped the deposition at the thickness of 0.10 nm, would be possible for γ-Al_2O_3. Since the thickness d_{mono} and the interlayer distance d_{layer} took nearly the same value (0.10 nm), the SLM of one monolayer stop was expected using TMA. As the lattice constant of the γ-Al_2O_3 is 0.794 nm, the obtained thicknesses of 0.08nm and 0.10nm are very small. This means that the one cycle of the TMA and H_2O could not form the unit cell of the γ-Al_2O_3. As shown in Fig. 2, however, the average interlayer distance d_{layer} is 0.10 nm and therefore the one cycle of the TMA and H_2O formed the one monolayer of the γ-Al_2O_3. From these results, the SLM of one monolayer stop was expected by using TMA as the source molecule.

Using the same method, the deposition rate of H_2O on the aluminum terminated Al_2O_3 was measured at the surface temperature of 1023 K. Before the adsorption process of H_2O, Al_2O_3 surface was exposed to the TMA. The TMA exposure time and the mole fraction were 5.0 s and 2.0×10^{-4} in the hydrogen carrier gas, respectively. This exposure corresponded to the surface collision of 2.0×10^{18} molecules cm^{-2}. Fig. 6 is the deposition rate as a function of the deposition thickness. Also in this case, the deposition was carried out through precursor-mediated adsorption, where the deposition rate R_{depo} kept nearly constant value up to the deposition thickness of 0.09 nm and then drastically decreased to zero.

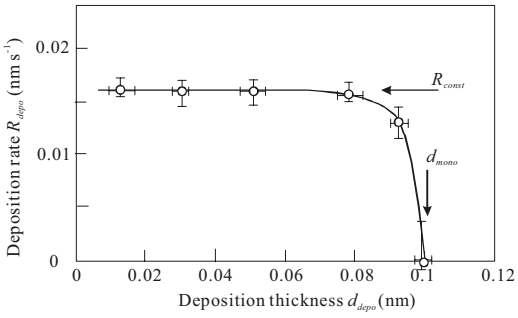

Fig. 6 Deposition thickness dependence of the deposition rate of oxygen. The similar behavior to the aluminum case (Fig. 5) was observed.

As shown in Fig. 2, the unit cell consists of four high-density layers and four low-density layers, which alternate along <001> direction. The theoretical and experimental studies have shown that the (001) surface termination of the γ-Al_2O_3 occurs along two kinds of faces, one terminated with the high-density plane, and another terminated with the low-density plane, although they are relaxed or reconstructed to take the minimum surface

energy [15-17]. The adsorption process on high-density surface is different from that on low-density surface. However, we were unable to distinguish them in the present experiment. If the adsorption of TMA was done on the high-density surface (N_{Al} = 6.3×10^{14} atom cm^{-2}), the constant deposition rate R_{const} 0.048 nm s^{-1} (see Fig. 5) was estimated to be R_{ads}=7.8×10^{-4} s^{-1} from Eq. (1). Such a small value was explained by a large amount of desorption of TMA from the surface. The small sticking coefficient has been reported in various semiconductors; for example, the sticking coefficients of O_2 on the Si(001) and Ge(001) surfaces range between 2.0×10^{-3} and 4.0×10^{-4}. It was expected in the present case that the growing surface was covered with a large amount of hydrogen, which inhibited the dissociation of TMA at the reaction site by the steric-hindrance effect.

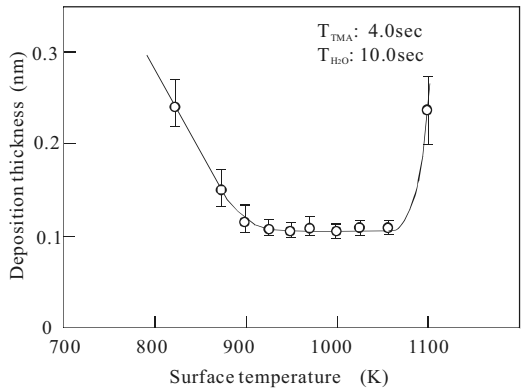

Fig. 7 Deposition rate of γ-Al_2O_3 as a function of the surface temperature. In the temperature range from 880K to 1050K, the deposition rate showed the same value of about 0.1 nm.

The surface temperature dependence of the deposition thickness was investigated from 800K to 1100K. The film growth was done under the growth condition of the pulse duration of 4.0 s of TMA (the mole fraction: 2.2×10^{-4}) and that of 10.0 s of H_2O (the mole fraction: 2.2×10^{-4}). Fig. 7 shows the deposition thickness variation as a function of the surface temperature. In the temperature range below 880K, the deposition thickness increased with decreasing the surface temperature. In this temperature range, the no SLM was observed and the growth rate increased even beyond 0.3 nm corresponding to 3 monolayers of γ-Al_2O_3. In the temperature range from 880K to 1050K, the deposition thickness was nearly constant (0.1 nm). As the surface was smooth in this temperature range, the ellipsometry allowed to measure the deposition thickness with small errors. In the temperature range above 1050K, the deposition rate again increased with increasing surface temperature. In this temperature range, we could not observe the deposition rate decreasing at a critical thickness. In this temperature range, the surface layer showed a very rough morphology and the thickness measurement by the ellipsometer was sometimes impossible. Therefore, the average of the thicknesses, which were measured for the samples showing the relatively smooth surface, was plotted in the figure.

(a) 760 K (b) 1020 K (c) 1050 K

Fig. 8 RHEED patterns of deposited films grown at 760 K, 1020 K and 1050 K. The ring pattern was observed for 760 K sample, the spotty for 1020 K sample and no pattern for 1050 K sample.

3.2. ALE of γ-Al_2O_3

Based on the adsorption data, the ALE of γ-Al_2O_3 was investigated using TMA and H_2O as the precursors of aluminum and oxygen, respectively. TMA and H_2O were alternatively supplied onto the surface with the hydrogen carrier gas. At first, the surface structure of the γ-Al_2O_3 grown in the temperature range from 880 K to 1050 K was studied by the RHEED measurement. In this experiment, the mole fractions of TMA and H_2O were 2.0×10^{-4}. The pulse durations of TMA and H_2O were 3.0 and 10.0 s, respectively. The gas cycle was 250 cycle. Fig. 8 shows the RHEED patterns of the Al_2O_3 films grown at 760 K, 1020 K, and 1050 K. The electron beam was injected along the [110] azimuth for the initial substrate GaAs(001) surface. The film grown at 760 K showed the ring pattern, suggesting that the polycrystalline or amorphous Al_2O_3 was grown (Fig.8 (a)). The similar RHEED pattern was observed for the Al_2O_3 grown below 880 K. The ALE was examined under various growth conditions in this temperature range but the RHEED pattern indicating a single crystal could not be observed. This probably came from the insufficient surface migration of source molecules (or precursors). The sufficient surface migration of source molecules is necessary to grow a single crystal but the low

surface temperature may cause the insufficient surface migration of source molecules. When the growth temperature was increased, the spotty pattern appeared instead of the ring pattern as shown in Fig. 8 (b). The spotty pattern indicated that the grown layer was crystalline. Assuming that the surface was 1×1 structure, the lattice constant was measured to be 0.794 nm from the distance between RHEED spots. This lattice constant was equal to the bulk lattice constant of γ-Al_2O_3 (0.795 nm) within the experimental error. Therefore, the grown layer was considered to have the crystal structure of γ-Al_2O_3. The spotty pattern was observed for the surface layers deposited in the temperature range from 900 K to 1050 K. When the growth temperature was further increased above 1050K, the spotty pattern disappeared and no RHEED patterns were observed on the screen. This was considered to be due to the surface coverage of aluminum liquid. When the surface temperature of Al_2O_3 was increased above 1050 K, the thermal-decomposition of TMA in the gas phase produced a lot of Al atoms on the growing surface, since the sticking coefficient of aluminum atom was nearly 1 in this temperature range. In this case, the growing surface would be covered with the Al droplets and therefore the Al_2O_3 ALE became impossible. In fact, the surface layer deposited at such high temperatures was found to be covered with the aluminum-dominated metal by the XMA measurement. From these results, the single crystalline γ-Al_2O_3 was grown in the temperature range from 900 K to 1050 K. The temperature dependence of the growth was consistent with that of the TMA adsorption (Fig. 7).

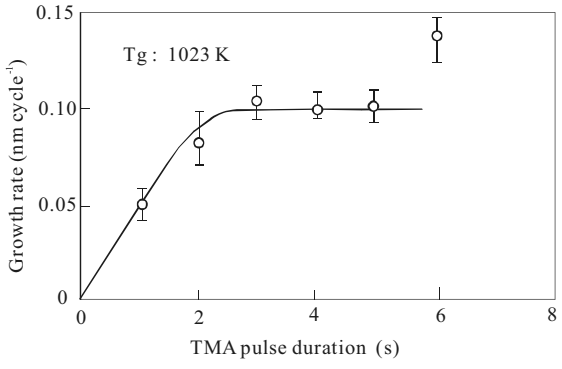

Fig. 9 TMA pulse duration dependence of the growth rate. A clear SLM was observed at the deposition thickness of one monolayer (0. 1nm).

Fig. 9 shows the variation of the growth rate as a function of the TMA pulse duration at the surface temperature of 1020 K. The growth experiments were carried out under the same supply condition of H_2O (the mole fraction of 2.0×10^{-4} and the pulse duration of 10.0 s). The growth rate increased with the pulse duration up to about 0.10 nm and then levels off for the pulse duration above 3.0 s. The surface morphology was atomically flat, if the TMA pulse duration was below 5 s. The saturation in the growth rate indicated the SLM at the thickness of 0.1 nm. However, for the pulse duration above 6 s, the growth rate drastically increased. The increase of growth rate was accompanied by the rough surface morphology of Al_2O_3 film. The deviation from the saturation in the growth rate was considered to be due to the appearance of the various crystal facets (the dominant facet is (111)), which caused the surface roughness and the uncontrollable adsorption of the source molecule. Although the phenomenon was not sufficiently understood, the supply of an excess of TMA probably changed the growth mode from two-dimensional growth to three-dimensional one. Once the droplet of aluminum appeared in the growing surface, the drastic change from two-dimensional growth to three-dimensional growth has been sometimes observed in the AlAs ALEs. The scanning electron microscopy (SEM) observation for the deposited layer deviated largely from the SLM indicated that the surface was covered with a lot of islands having the (111) facets. This suggested that the appearance of the (111) facets on the growing surface might cause the abnormal ALE.

The SLM usually appears when the surface reactivity for the source molecule changes from active to inactive. When the surface changes to completely inactive after the n monolayer deposition, an ideal SLM would be observed. However, the inactive surface sometimes changes to active due to the appearance of the highly reactive site on the growing surface. In this case, the ALE growth deviates from an ideal SLM. In many cases, the deviation from the SLM changes the epitaxial growth from two-dimensional to three-dimensional modes and then causes the surface roughness.

The H_2O pulse duration dependence of the growth rate was measured at the surface temperature of 1023 K. The H_2O of the mole fraction of 2.0×10^{-4} was used with hydrogen. The TMA supply condition was the mole fraction of 2.0×10^{-4} and the pulse duration of 5.0 s. Fig. 10

shows the variation of the growth rate as a function of the H_2O pulse duration. The growth rate increased with the pulse duration up to about 0.10 nm cycle^{-1} and then levels off for the pulse duration above 3.0 s. The surface morphology was atomically flat for the Al_2O_3 film grown below 15 s. The saturation in the growth rate indicated the appearance of the SLM. However, for the pulse duration above 20 s, the growth rate increased and the surface indicated the rough surface morphology. The deviation from the SLM was considered to be caused by the appearance of a lot of islands due to the uncontrollable adsorption of the source molecule as in the case of the excess TMA.

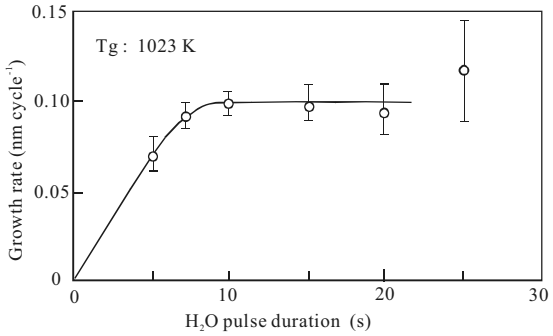

Fig. 10 H_2O pulse duration dependence of the growth rate. SLM was observed at the deposition thickness of one monolayer (0. 1 nm).

Until now, the ALEs having the ideal SLM have been reported in various III-V compounds, such as GaAs, InP and GaP. These compounds have a zinc blende structure and the SLM mechanism has been realized mainly for the crystal axis of <100>. The unit cell of the zinc blende structure is simply consisted of one type of tetrahedral, where the cation located in the center of an anion tetrahedral unit as shown in Fig. 2. When the ALE of the zinc blende crystal was carried out along the <001> direction, "two cycle" of source supply grew just one unit cell. For example, it was reported that the growth rate in the ALE of GaAs(001) was 0.28 nm cycle^{-1} which was just the half of the GaAs lattice constant 0.56 nm.

The γ-Al_2O_3 growth on (001) surface basically proceeds toward <001> direction. In the first step of this ALE, the TMA molecule is first adsorbed into a mobile, weakly bound precursor state (physisorption state). Some TMA molecules may migrate to the reaction sites and dissociate into Al atom and methyl bases. However, a larger amount of TMA cannot react on the growing surface and desorbs from the surface. The dissociated aluminum atoms are incorporated into the growing epitaxial layer. When the initial surface was consisted of the octahedrally coordinated layer, the dissociated Al atoms make a tetrahedrally coordinated layer. The theoretical calculation showed that the tetrahedrally coordinated surface largely relaxed and took a stable structure which involved the descent of the uppermost tetrahedral Al atoms in the bulk [15.16]. This energetically stable state was considered to prevent sticking of the excess of TMA under the proper growth condition and to indicate the SLM for TMA. In the second step of ALE, H_2O is adsorbed on the low-density tetrahedrally coordinated layer and the reaction between H_2O and the surface changes the tetrahedrally coordinated layer to the non-relaxed bulk-like structure and forms the octahedrally coordinated layer. In the third step, by the adsorption and the reaction of the TMA molecules supplied in the next cycle, construct the octahedrally coordinated layer is constructed. In the fourth step, H_2O pulse in the second gas cycle reacts with the Al atom, and the octahedrally coordinated layer was formed. Although the octahedrally surface indicate no large reconstruction, the relaxation of surface atoms occurs and the energetically stable structure appears on the surface. In the next step of the ALE, the above mentioned steps are repeated.

According to this model, the eight gas cycles (the one gas cycle: TMA and H_2O gas supplies), are necessary to grow the one unit cell of γ-Al_2O_3. This explains the growth rate of γ-Al_2O_3 ALE. From the ALE experiments as shown in Figs. 7 and 8, the deposition rate of 0.010 nm cycle^{-1} was obtained. The unit cell of γ-Al_2O_3 consists of 8 layers involving four octahedrally coordinated layers and four tetrahedrally coordinate layers. If the one gas cycle grows the one layer, the eight cycles may grow the film of 0.010× 8 = 0.80 nm, which nearly equals to the lattice constant of γ-Al_2O_3 (0.794 nm).

4. CONCLUSION

The TMA and H_2O were found to be effective precursors for the γ-Al_2O_3 ALE, when the surface was in the temperature range from 900 to 1050 K. They showed the clear SLM under the proper exposure durations and the mole fractions. On the assumption that the adsorption rate

was proportional to the deposition rate, it was concluded that these precursors were adsorbed through the precursor-mediated mechanism on the γ-Al_2O_3 surface. The very slow adsorption rate of the order of 10^{-4} s was considered to be due to the steric-hindrance effect of the hydrogen molecules adsorbed on the growing surface. The growth rate of the γ-Al_2O_3 ALE was explained by the adsorptions of the TMA and H_2O on the energetically stable surface layers.

References

[1] Y. Xuan, H. C. Lin, P. D. Ye, G. D. Wilk, Appl. Phys. Lett. 88 (2006) 263518.

[2] H. Zhao, D. Shahrjerdi, F. Zhu, M. Zhang, H. Kim, I. OK, J. H. Yum, S. Park, S. K. Banerjee, J. C. Lee, Appl. Phys. Lett. 92 (2008) 233508.

[3] T. D. Lin, H. C. Chiu, P. Chang, L. T. Tung, C. P. Chen, M. Hong, J. Kwo, W. Tsai, Y.C. Wang, Appl. Phys. Lett. 93 (2008) 033516.

[4] M. Ozeki, Mater. Sci. Rept. 8 (1992) 97.

[5] S. M. Bedair, B. T. McDermott, Y. Ide, N. H. Karam, H. Hashemi, M. A. Tischler, M. Timmons, J. C. L. Taran, N. A. El-Masry, J. Crystal Growth 93 (1988) 182.

[6] J. Nishizawa, H. Abe, T. Kurabayashi, J. Electrochem. Soc. 132 (1985) 1197.

[7] A. Doi, Y. Aoyagi, S. Namba, Appl. Phys. Lett. 48 (1986) 1787.

[8] M. Ozeki, K. Mochizuki, N. Ohtsuka, K. Kodama, Appl. Phys. Lett. 16 (1988) 1509.

[9] Y. Sakuma, M. Ozeki, N. Ohtsuka, K. Kodama, J. Appl. Phys. 69 (1990) 5660.

[10] F. H. Streitz, J. W. Mintmire, Phys. Rev. B 60 (1999) 773.

[11] M. M. Frank, G. D. Wilk, D. Starodub, T. Gustafsson, E. Garfunkel, Y. J. Chabal, J. Grazul, D. A. Muller, Appl. Phys. Lett. 86 (2005) 152904.

[12] C. H. Chang, Y. K. Chiou, Y. C. Chang, K. Y. Lee, T. D. Lin, T. B. Wu, M. Hong, J. Kwo, Appl. Phys. Lett. 89 (2006) 242911.

[13] C. W. Cheng, E. A. Fitzgerald, Appl. Phys. Lett. 93 (2008) 031902.

[14] F. Ren, J. M. Kuo, M. Hong, W. S. Hobson, J. R. Lothian, J. Lin, H. S. Tsai, J. P. Mannaerts, J. Kwo, S. N. G. Chu, Y. K. Chen, A.Y. Cho, IEEE Electron Device Lett. 19 (1998) 309.

[15] A. Vijay, G. Mills, H. Metiu, J. Chem. Phys. 117 (2002) 4509.

[16] H. P. Pinto, R. M. Nieminen, S. Elliott, Phys. Rev. B 70 (2004) 125402.

[17] P. Nortier, P. Fourre, A. B. Mohammed Saad, O. Saur, J. C. Gavalley, Appl. Catal. 61 (1990) 161.